

Theory of Raman response in a superconductor with extended s -wave symmetry: Application to Fe-pnictides

Andrey V. Chubukov,¹ Ilya Eremin,^{2,3} and Maxim M. Korshunov^{2,4}

¹*Department of Physics, University of Wisconsin-Madison, Madison, WI 53706, USA*

²*Max-Planck-Institut für Physik komplexer Systeme, D-01187 Dresden, Germany*

³*Institute für Mathematische und Theoretische Physik,*

TU Braunschweig, D-38106 Braunschweig, Germany

⁴*L. V. Kirensky Institute of Physics, Siberian Branch of Russian Academy of Sciences, 660036 Krasnoyarsk, Russia*

(Dated: October 27, 2018)

We argue that Raman study of Fe-pnictides is a way to unambiguously distinguish between various superconducting gaps proposed for these materials. We show that A_{1g} Raman intensity develops a true resonance peak below 2Δ if the pairing gap has A_{1g} symmetry in the folded Brillouin zone ($\Delta(k=0) = \Delta$, $\Delta(\pi, \pi) = -\Delta$). No such peak develops for a pure s -wave gap, a d -wave gap, and an extended s -wave gap with $\Delta(\mathbf{k}) = \Delta \cos \frac{k_x}{2} \cos \frac{k_y}{2}$. We show that the peak remains quite strong for the values of inter-pocket impurity scattering used to fit NMR data.

PACS numbers: 74.20.Mn, 74.20.Rp, 74.25.Jb, 74.25.Gz

Recent discovery of superconductivity in the iron-based layered pnictides with T_c reaching 55K generated an enormous interest in the physics of these materials¹. Most of ferropnictides are quasi two-dimensional materials, and their parent (undoped) compounds are metals and display antiferromagnetic long-range order below $T_N \sim 150\text{K}$ ^{1,2,3}. Superconductivity occurs upon doping of either electrons or holes into FeAs layers, or by applying pressure. The electronic structure measured by angle-resolved photoemission (ARPES)⁴ and by magneto-oscillations⁵ consists of two small hole pockets centered around the $\Gamma = (0, 0)$ point and two small electron pockets centered around the $M = (\pi, \pi)$ point in the folded Brillouin zone (BZ). The sizes of electron and hole pockets are about equal in parent compounds.

The key unresolved issue for the pnictides is the symmetry of the superconducting gap. A conventional phonon-mediated s -wave superconductivity is unlikely because electron-phonon coupling calculated from first principles is quite small⁶. Several authors considered magnetically mediated pairing based either on itinerant^{7,8,9} or localized spin models¹⁰ and argued that the gap should have an extended s -wave symmetry $\cos k_x + \cos k_y$ (also called s^+ or, equivalently, A_{1g} symmetry). This gap changes sign between hole and electron pockets but has no nodes along the Fermi surface (FS). On the other hand, another RPA study of magnetically mediated superconductivity in the five-band Hubbard model¹¹ yielded two nearly degenerate candidate states in which the gap has nodes on one of the FS sheets: either an extended s -wave state with $\Delta(\mathbf{k}) \approx \Delta \cos \frac{k_x}{2} \cos \frac{k_y}{2}$, or a $d_{x^2-y^2}$ state with $\Delta(\mathbf{k}) \approx \Delta \sin \frac{k_x}{2} \sin \frac{k_y}{2}$ (in the unfolded BZ, these two states are $\cos q_x + \cos q_y$ and $\cos q_x - \cos q_y$, respectively¹²).

The experimental situation is also controversial. ARPES^{15,16} and Andreev spectroscopy¹⁷ measurements have been interpreted as evidence for a nodeless gap, either pure s -wave or s^+ -wave. The resonance observed in

neutron measurements¹⁸ is consistent with the s^+ gap¹⁹. On the other hand, nuclear magnetic resonance (NMR) data²⁰ and some of penetration depth data²¹ were interpreted as evidence for the nodes in the gap. Some, but not all of the data can be reasonably fitted by a model of an s^+ SC with ordinary impurities^{14,22,23}.

In view of both theoretical and experimental uncertainties, it is important to find measurements which could unambiguously distinguish between different pairing symmetries. Recent suggestions for such probes include Andreev bound state²⁴ and Josephson interferometry²⁵. In this communication, we argue that the study of A_{1g} Raman intensity is another way to determine the symmetry of the superconducting gap. We show that in the A_{1g} scattering geometry the Raman signal develops a true resonance below 2Δ for the case of s^+ gap. No such resonance appears for a pure s -wave gap, for $\cos \frac{k_x}{2} \cos \frac{k_y}{2}$ and $\sin \frac{k_x}{2} \sin \frac{k_y}{2}$ gaps. The A_{1g} resonance is the effect of the final state interaction, which is known to be important for Raman scattering²⁶. A similar resonance occurs in the B_{1g} channel in a magnetically mediated $d_{x^2-y^2}$ superconductor²⁷, but there the resonance is weakened by a finite damping associated with nodes of the d -wave gap.

We model Fe-pnictides by an itinerant electron system with two (almost) degenerate hole FS pockets centered at the Γ point and two electron FS pockets centered at the M point. We assume that the magnitude of the gap Δ is much smaller than the Fermi energy. In this situation, Raman intensity at frequencies $\leq 2\Delta$ is determined by states near the FS where the density of states (DOS) can be approximated by a constant. We first assume that the pairing gap has s^+ symmetry, $\Delta(\mathbf{k} \approx 0) = \Delta$, $\Delta(\mathbf{k} \approx \pi) = -\Delta$, and show how the resonance appears. We then discuss other pairing symmetries.

Without final state interaction, the Raman intensity in a clean BCS s^+ superconductor is the same as in a pure s -wave superconductor²⁶ and is given by $I_i(\Omega) =$

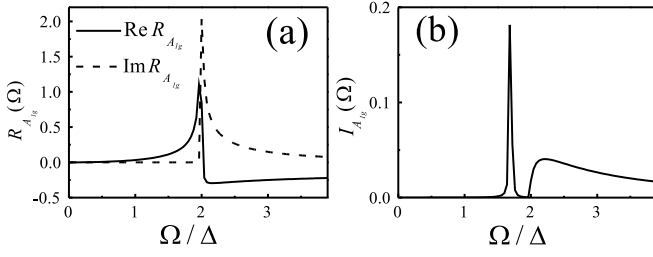


FIG. 1: Real and imaginary parts of the A_{1g} Raman intensity for a clean s^+ superconductor without (a) and with (b) final state interaction. Final state interaction gives rise to a well-defined resonance in the A_{1g} intensity. We used $R_0 = 1/(4\pi)$, $u_{eff}R_0 \approx 0.4$, and added damping $\gamma = 0.001\Delta$.

$2\text{Im}R_i(\Omega)$, where

$$R_{A_{1g}}(\Omega) = -R_0 \left\langle \int d\omega \gamma_{A_{1g}}^2 \left[1 - \frac{\omega_+ \omega_- - \Delta^2}{\sqrt{\omega_+^2 - \Delta^2} \sqrt{\omega_-^2 - \Delta^2}} \right] \times \frac{1}{\sqrt{\omega_+^2 - \Delta^2} + \sqrt{\omega_-^2 - \Delta^2}} \right\rangle_{FS}$$

Here $\gamma_{A_{1g}} = \cos k_x + \cos k_y$ is the geometrical factor for A_{1g} scattering, $\omega_{\pm} = \omega \pm \Omega/2$, and $\langle \dots \rangle_{FS}$ denotes the averaging over FS. The factor 2 in the relation between $I_i(\Omega)$ and $R_i(\Omega)$ reflects the fact that there are two hole and two electron pockets. Other factors are incorporated into R_0 .

The intensity $I_{A_{1g}}(\Omega)$ computed using (1) vanishes at $\Omega < 2\Delta$ and is discontinuous at 2Δ . The real part of $R_{A_{1g}}$, which we will need later, is positive below 2Δ , scales as Ω^2 at small frequencies, and diverges upon approaching 2Δ from below²⁸. We show both $\text{Re}R_{A_{1g}}$ and $\text{Im}R_{A_{1g}}$ in Fig. 1. The final state interaction is diagrammatically represented as the renormalization of the Raman vertex. Vertex corrections arise from multiple insertions of fermion-fermion interactions into the Raman bubble. There are five different interactions between low-energy fermions (see Fig. 2(a)). They include intra-band interactions for electrons (u_4) and for holes (u_5), which we assume to be equal, inter-band interactions u_1 and u_2 with momentum transfer 0 and (π, π) , respectively, and the pair hopping term u_3 .

A generic theory of vertex renormalizations has been developed in Ref.²⁶ and we follow this work in our analysis. In general, there are three different types of vertex corrections: (i) the corrections which come from short-range interactions u_i and transform a bare A_{1g} Raman vertex into a renormalized *particle-hole* vertex (these corrections involve GG and FF bubbles, where G and F are normal and anomalous Green's functions), (ii) the corrections which transform a Raman vertex into a *particle-particle* vertex (these involve GF bubbles) (see Fig. 2(b)), and (iii) the corrections from the long-range component of the Coulomb interaction $V_q \propto 1/q^2$. The

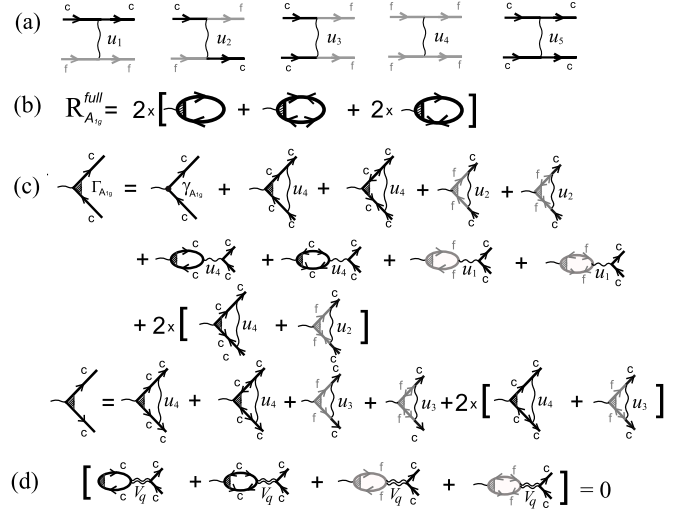


FIG. 2: (a) Five relevant interactions between fermions near hole and electron FS pockets. Black and grey lines represent fermionic c -states near $(0,0)$ and f -states near $M = (\pi, \pi)$. (b) The full Raman bubble, which is the sum of GG , FF and GF terms. Only the contribution from c -fermions is shown. (1) The one from f -fermions is obtained by replacing c lines by f -lines and vice versa in (b) and (c) panel. (c) The renormalization of the A_{1g} Raman vertex for c -fermions. The first 8 diagrams account for “conventional” renormalization of the A_{1g} particle-hole vertex and involve GG and FF bubbles, the last two diagrams involve GF bubbles and emerge due to a non-zero coupling between A_{1g} particle-hole channel and ordinary s -wave pairing channel. The renormalization of the particle-particle vertex in turn involves 4 “conventional” diagrams with GG and FF terms, which account for the renormalization in the particle-particle channel, and two diagrams due to the coupling to the A_{1g} particle-hole channel. (d) The renormalizations due to long-range component of Coulomb interaction $V_q \propto 1/q^2$. This renormalization vanishes because of the symmetry between c - and f -fermions and the fact that $\gamma_{A_{1g}}(k=0) = -\gamma_{A_{1g}}(\pi)$.

corrections of the first type are given by ladder and bubble diagrams which involve u_1 , u_2 and u_4 vertices (first 8 terms in Fig. 2(c)). The corrections of the second-type are non-zero when the symmetry of the gap is the same as the symmetry of the Raman vertex, which is our case. These corrections transform A_{1g} particle-hole vertex into an ordinary s -wave pairing vertex (the terms with the overall factor 2 in Fig. 2 (c)). The third renormalization, due to long-range component of the Coulomb interaction, generally gives rise to a screening of the Raman signal^{26,29}, but vanishes in our case because of particle-hole symmetry and the fact that A_{1g} Raman vertex $\gamma_{A_{1g}}$ changes sign between hole and electron pockets (see Fig. 2(d)). Note in this regard that $V_q \propto 1/q^2$ is not a part of RG transformation and depends only on a momentum transfer q , in distinction to the other two interactions with small momentum transfer, u_4 and u_1 . The bare values of u_4 and u_1 may be identical, but the two flow in different directions under RG. Also note that we did

not include a momentum-independent term into $\gamma_{A_{1g}}$. If $\gamma_{A_{1g}}$ had such component, it would be screened by the long-range Coulomb interaction.

Combining the renormalizations (i) and (ii) and evaluating the diagrams, we obtain the full Raman intensity $I_{A_{1g}}^{full}(\Omega) = 2\text{Im}R_{A_{1g}}^{full}(\Omega)$ with $R_{A_{1g}}^{full}(\Omega)$ in the form

$$R_{A_{1g}}^{full}(\Omega) = \frac{R_{A_{1g}}(\Omega)(1 + u_f R_{pp}(\Omega)) + 4u_f R_{mix}^2(\Omega)}{(1 - u_{eff} R_{A_{1g}}(\Omega))(1 + u_f R_{pp}(\Omega)) - 4u_g u_f R_{mix}^2(\Omega)}, \quad (2)$$

where $u_{eff} = 2u_1 - u_2 - u_4$ is the effective vertex for the Raman renormalization in the A_{1g} particle-hole channel, $u_f = u_3 + u_4$, $u_g = u_4 - u_2$, $R_{pp}(\Omega) \propto \log E_F/\Omega > 0$ is the polarization bubble in the s -wave particle-particle channel, and $R_{mix}(\Omega) \propto \int d^2k d\omega \gamma_{A_{1g}} G_{k,\omega+\Omega} F_{k,\omega}$ couples A_{1g} particle-hole channel and s -wave particle-particle channel. At low frequencies, $R_{mix}(\Omega) \propto \Omega$. In this respect, the situation is similar to the case of a spin resonance in a d -wave superconductor, where $S = 1$ particle-hole channel couples to $S = 0$ particle-particle channel³¹.

Because s -wave channel is repulsive in our case ($u_3 + u_4 > 0$), there is no pole in $R_{A_{1g}}^{full}(\Omega)$ coming from the particle-particle channel. Furthermore, $R_{pp}(\Omega)$ logarithmically diverges at $\Omega \ll E_F$, and canceling this divergent term between the numerator and the denominator in (2), we obtain

$$I_{A_{1g}}^{full}(\Omega) \approx 2 \frac{\text{Im}R_{A_{1g}}}{(1 - u_{eff} \text{Re}R_{A_{1g}})^2 + (u_{eff} \text{Im}R_{A_{1g}})^2}. \quad (3)$$

We see therefore that the coupling between A_{1g} particle-hole and s -wave particle-particle channels is irrelevant, and the full $I_{A_{1g}}^{full}(\Omega)$ can be approximated by the expression which only includes vertex corrections which preserve particle-hole structure of the Raman vertex.

Our next observation is that for two-band structure, u_{eff} contains the terms u_1 and u_2 , which do not contribute to the renormalization of the s^+ pairing vertex (the latter involves u_3 and u_4 terms¹⁴), i.e., in distinction to one-band case²⁶, the renormalization of the A_{1g} Raman vertex and the renormalization of the s^+ pairing vertex (which has the same A_{1g} symmetry) are given by different combinations of the interactions u_i .

Finally, we note that below 2Δ , $\text{Im}R_{A_{1g}} = 0$ while $\text{Re}R_{A_{1g}}$ is positive and evolves between zero and infinity when Ω changes between zero and 2Δ . Then, for positive u_{eff} , the A_{1g} Raman intensity develops a δ -functional resonance peak below 2Δ , at a frequency where $u_{eff} \text{Re}R_{A_{1g}} = 1$. For a $d_{x^2-y^2}$ superconductor the same effect leads to an excitonic resonance in a staggered spin susceptibility³⁰, and to a pseudo-resonance in a B_{1g} Raman response²⁷.

The flow of the interactions between the bandwidth W and the Fermi energy E_F has been analyzed in the earlier RG study¹⁴, and the result is that u_1 becomes the largest

interaction at energies comparable to the Fermi energy, even if the intra-band Hubbard repulsion u_4 is the largest term in the Hamiltonian. Specifically, in the RG flow u_1 and u_3 increase, u_2/u_1 flows to zero, and the u_4 term decreases, such that $u_{eff} = 2u_1 - u_4 - u_2$ becomes positive at energies below E_F , relevant to Raman scattering, and *the A_{1g} Raman response develops a resonance below 2Δ* . We emphasize that the physics which makes u_{eff} positive is the same physics that gives rise to an attraction in an extended s^+ -wave pairing channel. Indeed, the pairing interaction in s^+ channel, which is the combination $u_3 - u_4$, becomes positive under RG.

For other proposed gap symmetries, the resonance does not develop, even if one neglects the screening by long-range Coulomb interaction. For an s -wave gap, there is no sign change between electron and hole FS, and the analog of u_{eff} in Eq. (3) is $-2u_1 - u_4 + u_2$. This combination is negative, so the resonance does not occur. For a gap that changes sign along either hole or electron FS, the largest contribution to $I_{A_{1g}}(\Omega)$ comes from the FS along which the gap is nodeless. Vertex renormalization for such term contains $-u_4 + (2u_1 - u_2)x$, where $x \sim k_F^2$, and k_F is a small radius of the FS along which the gap has nodes. In this situation, u_1 term does not overcome u_4 , and the resonance does not occur. For d_{xy} gap⁹ with $\Delta \propto \sin k_x \sin k_y$ (in the folded BZ), all u_i terms in the vertex renormalization are reduced. Resonance may still occur, but the effective interaction now is small, $O(k_F^2)$, and the resonance is washed out by a small damping. This shows that the A_{1g} Raman resonance is a fingerprint of an s^+ pairing.

Finally, we consider how the resonance in s^+ superconductor is affected by ordinary impurities. As in earlier works^{14,23}, we introduce impurity potential $U_i(q)$ with intra- and inter-pocket terms $U_i(0)$ and $U_i(\pi)$, respectively and restrict with the Born approximation. This approximation (which requires $U_i \ll E_F$) may not work for $U_i(0)$ (Ref.²²) but should be valid for $U_i(\pi)$ which is pair-breaking and is therefore very likely not larger than $\Delta \ll E_F$. For our case, $U_i(0)$ controls the functional form of $\text{Re}R_{A_{1g}}$, which still evolves between zero and infinity when Ω changes between 0 and 2Δ , while the broadening of the resonance is entirely due to $U_i(\pi)$. In this situation, Born approximation should be sufficient.

The calculations are straightforward and we refrain from presenting the details. Intra-pocket impurity scattering does not affect the gap by Anderson's theorem, but $U_i(\pi)$, which scatter fermions with $+\Delta$ and $-\Delta$, is pair-breaking and affects the gap in the same way as magnetic impurities in an ordinary s -wave superconductor. We use $b = 2U_i(\pi)/\Delta$, where Δ is the order parameter as a measure of the strength of pair-breaking impurity scattering.

The results of the calculations are shown in Fig. 3, where we plot Raman intensity in the presence of impurities both without and with final state interaction. Comparing this figure with Fig. 1 we see that the resonance gets damped at a finite b , and Raman intensity

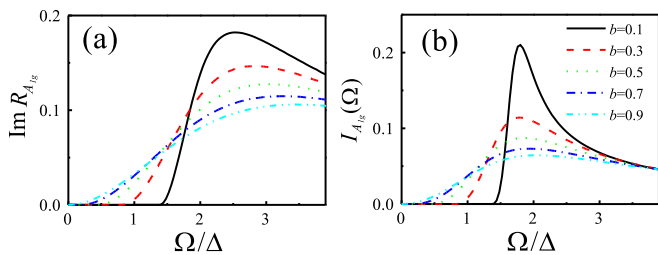


FIG. 3: (color online) Calculated Raman intensity for an s^+ superconductor without (a) and with (b) final state interaction for various strength of the inter-band impurity scattering. We use the same u_{eff} as in Fig. 1 and for definiteness set $U_i(0) = \Delta$.

no longer shows two peaks. Still, the resonance continue to determine the shape of $I_{A_{1g}}(\Omega)$: without final state interaction the peak broadens and shifts to larger frequencies $\Omega > 2\Delta$ upon increasing b , while when the final state interaction is included, the peak remains below 2Δ and shifts to a smaller frequency with increasing b . Notice that the resonance is still quite strong at $b \sim 0.5-0.7$, which was used to fit NMR and penetration depth data^{14,23}. In other words, it should be observable

in Raman experiments if indeed the gap has an s^+ symmetry.

To conclude, in this paper we argued that Raman study of Fe-pnictides is a way to unambiguously distinguish between various superconducting gaps proposed for these materials. We have shown that for an A_{1g} (s^+) gap $\Delta(\mathbf{k} \approx 0) = \Delta$, $\Delta(\mathbf{k} \approx \pi) \approx -\Delta$, the A_{1g} Raman intensity has a true resonance peak below 2Δ . No such peak emerges for a pure s -wave gap, a $d_{x^2-y^2}$ gap, and an extended s -wave gap with $\Delta(\mathbf{k}) = \Delta \cos \frac{k_x}{2} \cos \frac{k_y}{2}$. The resonance peak gets broader by pair-breaking inter-pocket impurity scattering but is still fairly visible for the values of impurity scattering used to fit NMR data.

We acknowledge useful conversations with G. Blumberg, W. Brenig, H.-Y. Choi, D.V. Efremov, A. Sacuto, M. Vavilov, A. Vorontsov. A.V.C. acknowledges support from nsf-dmr 0604406. I.E. acknowledges partial support from the Asian-Pacific Center for Theoretical Physics, the Volkswagen Foundation (I/82203) and the Program "Development of scientific potential of a higher school" (N1 2.1.1/2985). M.M.K. acknowledges support from RFBR 07-02-00226, OFN RAS program on "Strong electronic correlations", and RAS program on "Low temperature quantum phenomena".

-
- ¹ Y. Kamihara, T. Watanabe, M. Hirano, and H. Hosono, *J. Am. Chem. Soc.* **130** 3296 (2008).
 - ² Clarina de la Cruz *et al.*, *Nature* **453**, 899 (2008).
 - ³ H.-H. Klauss *et al.*, *Phys. Rev. Lett.* **101**, 077005 (2008).
 - ⁴ C. Liu *et al.*, *Phys. Rev. Lett.* **101**, 177005 (2008); D.V. Evtushinsky *et al.*, arXiv:0809.4455 (unpublished); D. Hsieh *et al.*, arXiv:0812.2289 (unpublished); H. Ding *et al.*, arXiv:0812.0534 (unpublished).
 - ⁵ A.I. Coldea *et al.*, *Phys. Rev. Lett.* **101**, 216402 (2008).
 - ⁶ L. Boeri, O. V. Dolgov, A. A. Golubov, *Phys. Rev. Lett.* **101**, 026403 (2008).
 - ⁷ I.I. Mazin, D.J. Singh, M.D. Johannes, and M.H. Du, *Phys. Rev. Lett.* **101**, 057003 (2008).
 - ⁸ Y. Yanagi, Y. Yamakawa, and Y. Ono, *J. Phys. Soc. Jpn.* **77** 123701 (2008); H. Ikeda, *J. Phys. Soc. Jpn.* **77**, 123707 (2008).
 - ⁹ S.-L. Yu, J. Kang, and J.-X. Li, arXiv:0901.0821 (unpublished).
 - ¹⁰ M. M. Parish, J. Hu, and B. A. Bernevig, *Phys. Rev. B* **78**, 144514 (2008).
 - ¹¹ S. Graser, T. A. Maier, P. J. Hirschfeld, D. J. Scalapino, arXiv:0812.0343 (unpublished).
 - ¹² Strictly speaking, the extended s -wave states with $\Delta(\mathbf{k}) \propto \cos k_x + \cos k_y$ and $\Delta(\mathbf{k}) \propto \cos \frac{k_x}{2} \cos \frac{k_y}{2}$ cannot be decoupled in the gap equation as both are members of the A_{1g} representation of D_{4h} tetragonal space group. However, for small hole and electron pockets, the matrix element between the two is small.
 - ¹³ F. Wang, H. Zhai, Y. Ran, A. Vishwanath, and D.-H. Lee, *Phys. Rev. Lett.* **102**, 047005 (2009).
 - ¹⁴ A.V. Chubukov, D.V. Efremov, and I. Eremin, *Phys. Rev. B* **78**, 134512 (2008).
 - ¹⁵ T. Kondo *et al.*, *Phys. Rev. Lett.* **101**, 147003 (2008).
 - ¹⁶ H. Ding *et al.*, *Europhys. Lett.* **83**, 47001 (2008).
 - ¹⁷ T. Y. Chen, Z. Tesanovic, R. H. Liu, X. H. Chen, C. L. Chien, *Nature* **453**, 1224 (2008).
 - ¹⁸ A.D. Christianson *et al.*, *Nature* **456**, 930 (2008); M.D. Lumsden *et al.*, arXiv:0811.4755 (unpublished).
 - ¹⁹ M.M. Korshunov and I. Eremin, *Phys. Rev. B* **78**, 140509(R) (2008); T.A. Maier and D.J. Scalapino, *Phys. Rev. B* **78**, 020514(R) (2008).
 - ²⁰ Y. Nakai, K. Ishida, Y. Kamihara, M. Hirano, and H. Hosono, *J. Phys. Soc. Jpn.* **77**, 073701 (2008); K. Matano *et al.*, *Europhys. Lett.* **83**, 57001 (2008); H.-J. Grafe *et al.*, *Phys. Rev. Lett.* **101**, 047003 (2008).
 - ²¹ R.T. Gordon *et al.*, arXiv:0810.2295 (unpublished); R.T. Gordon *et al.*, arXiv:0812.3683 (unpublished); J.D. Fletcher *et al.*, arXiv:0812.3858 (unpublished).
 - ²² D. Parker, O.V. Dolgov, M.M. Korshunov, A.A. Golubov, and I.I. Mazin, *Phys. Rev. B* **78**, 134524 (2008).
 - ²³ Y. Bang, H.-Y. Choi, and H. Won, arXiv:0808.3473 (unpublished); Y. Senga and H. Kontani, *J. Phys. Soc. Jpn.* **77**, 113710 (2008); A.B. Vorontsov, M.G. Vavilov, and A.V. Chubukov, arXiv:0901.0719 (unpublished).
 - ²⁴ P. Ghaemi, F. Wang, and A. Vishwanath, arXiv:0812.0015 (unpublished).
 - ²⁵ D. Parker and I. Mazin, arXiv:0812.4416 (unpublished); J. Wu and Ph. Phillips, arXiv:0901.0038 (unpublished).
 - ²⁶ M.V. Klein and S.B. Dierker, *Phys. Rev. B* **29**, 4976 (1984). See also W. Wu and A. Griffin, *Phys. Rev. B* **52**, 7742 (1995); T. P. Devereaux and D. Einzel, *Phys. Rev. B* **51**, 16336 (1995); T. Strohm and M. Cardona, *Phys. Rev. B* **55**, 12725 (1997).
 - ²⁷ A. Chubukov, D. Morr, and G. Blumberg, *Solid State Comm.* **112**, 193 (1999); A. V. Chubukov, T. P. Devereaux, and M. V. Klein, *Phys. Rev. B* **73**, 094512 (2006).

- ²⁸ A. V. Chubukov and M.R. Norman, Phys. Rev. B **77**, 214529 (2008). Note that in this paper the irreducible vertex $\Gamma_{\alpha\beta,\gamma\delta}$ has opposite sign compared to our interaction potentials u_i .
- ²⁹ A. Abrikosov and V.M. Genkin, Sov. Phys. JETP **38**, 417 (1974).
- ³⁰ see, e.g., M. Eschrig, Adv. Phys. **55**, 47 (2006).
- ³¹ O. Tchernyshov, M.R. Norman, and A.V. Chubukov, Phys. Rev. B **63**, 144507 (2001); W.C. Lee, J. Sinova, A.A. Burkov, Y. Joglekar, and A.H. MacDonald, Phys. Rev. B **77**, 214518 (2008); Z. Hao and A. Chubukov, arXiv:0812.2697 (unpublished).